The following publication H. F. Wong et al., "Gate-Controlled Transport Properties in Dilute Magnetic Semiconductor (Zn, Mn)O Thin Films," in IEEE Transactions on Magnetics, vol. 54, no. 11, pp. 1-4, Nov. 2018, Art no. 4200104 is available at https://doi.org/10.1109/TMAG.2018.2850067

Gate-controlled Transport Properties in Dilute Magnetic Semiconductor (Zn, Mn)O Thin Films

H.F. Wong[1], S.M. Ng[1], Y.K. Liu[1], K.K. Lam[1], K.H. Chan[1], W.F. Cheng[1], D. von Nordheim[2], C.L. Mak[1], B. Ploss[2] and C.W. Leung[1]

[1]Department of Applied Physics, The Hong Kong Polytechnic University, Hung Hom, Kowloon, Hong Kong
[2]Department of SciTec, University of Applied Sciences Jena, Carl-Zeiss-Promenade 2, 07743 Jena, Germany

Ionic liquid (IL) gating of functional oxides has drawn significant attentions, since it can provide reversible changes in carrier concentration (~10^{14} cm^{-3}) at the interface, permitting the manipulation of electrical and magnetic properties of oxide films with low voltages. In this work, we demonstrated the electric-field manipulation of transport properties in dilute magnetic oxide (DMS) of $Zn_{0.98}Mn_{0.02}O$ (MZO) using an electric-double-layer transistor (EDLT) geometry through the ionic liquid electrolyte. The MZO EDLTs exhibited a reversible control of resistance up to 33 % at 230 K. Moreover, magnetoresistance (MR) measurement revealed the influence of gate voltage (V_g) on the magnetotranspsort behavior, which exhibited a positive MR in the low field region and a negative-MR in high magnetic field (up to 9 T). An increase in low-field positive MR (<1 T) upon switching the V_g from -2 to 2 V implied an enhanced ferromagnetic state of MZO due to increased electron carrier concentration. The present results therefore demonstrated controllable carrier concentration by electric-field effect plays an important role in the manipulation of magnetism in MZO.

***Index Terms*— Electric effect, Mn-doped ZnO, DMS and magnetism**

I. Introduction

ELECTRIC-FIELD manipulation of magnetic properties provides a promising way for preparing fast and compact data storage devices [1-4]. Recently, intensive studies are made on the control of magnetism in artificial multiferroic heterostructures through the manipulation of charge carriers or inducing strains [4-11]. However, these heterostructure are often limited by the compatibility between the ferromagnetic and ferroelectric components, such as lattice mismatching issue and interfacial diffusion due to high deposition temperatures [7, 11]. Moreover, for observable tunability of magnetism one often requires thin ferroelectric layers or large-switching voltages for complete reversal of the polarization directions [12], and often results in the breakdown of the ferroelectric layer [6].

For low-switching voltages and highly tunability of carrier concentrations in the ferromagnetic interface, ionic-liquid (IL)-gating modulation has demonstrated interfacial carrier concentration changes up to 10^{14} cm^{-2} in ferromagnets, which is even larger than the tuning by electrostatic doping via magnetoelectric coupling [13-17]. The ionic-liquid-gating technique has been widely deployed for achieving high tunability in different systems such as metal-to-insulator transition in the complex oxides [13, 14], controlling superconductivity behavior in two-dimensional materials [18] and exchange-bias effect in antiferromagnets [19].

Generally, the electric-field control of carrier density is more effective in manipulating semiconductor as compared metallic systems, since the carrier density in semiconductors is 2-3 order of magnitude smaller [1]. A high tunability in carrier density is expected as the screening depth is increased. Among the candidates of ferromagnetic semiconductors, manganese-substituted zinc oxide (MZO) has the advantage that the carrier concentration is independent of the total moment of MZO film since the zinc atom is isovalent with manganese [20]. Previous studies have shown that the magnetic moment of MZO can be controlled via manganese doping or the oxygen content inside the film [20, 21].

In this work, we report the fabrication and characterization of electric-double-layer transistors (EDLTs) for electric-field manipulation of magnetotranspsort in *n*-type MZO. The devices were characterized by several techniques, including X-ray diffractometry (XRD), atomic force microscopy (AFM), Hall measurements, resistance–switching tests and magnetotranspsort measurements. Our results showed the gate voltage (V_g) manipulation in the accumulations and depletion of charge carriers of the MZO films through a low magnitude ($\leq$ 2V) V_g. Moreover, our results also demonstrate that the low-temperature magnetotranspsort in MZO can be manipulated by V_g.

II. Experimental Procedure

10 nm-thick $Zn_{0.98}Mn_{0.02}O$ (hereafter MZO) thin films were deposited on (0001) Al_2O_3 single crystal substrates by pulsed laser deposition. The film deposition was performed at 300ºC with an oxygen pressure of 5 x10^{-4} Pa. The as-grown films were cooled down to room temperature in the same oxygen ambient at a rate of ~10ºC/min for promoting the oxygen stoichiometry of the deposited films. Thickness of as-grown films was estimated by the number of laser pulses used and was further confirmed with AFM.

For electric-field manipulation of MZO devices, the films were patterned into Hall-bars (channel width: 50 μm, channel length: 110 μm) by photolithography and wet etching, using dilute HCl (1%HCl, etching rate: 60 nm/mins) as etchant [22]. Fig. 1(a) depicts the schematic of the device employed in this

Manuscript received April 1, 2015; revised May 15, 2015 and June 1, 2015; accepted July 1, 2015. Date of publication July 10, 2015; date of current version July 31, 2015. Corresponding author: C. W. Leung (e-mail: apleung@polyu.edu.hk). Color versions of one or more of the figures in this paper are available online at http://ieeexplore.ieee.org. Digital Object Identifier (inserted by IEEE).

study. The MZO thin film Hall bar devices were capped by 2 nm of SiO_2 to prevent the direct contact between the MZO film and the IL electrolyte (N, N-diethyl-N-(2methoxyethyl)-N-methylammonium-bis-(trifluoromethylsulfonyl)-imide, DEME-TFSI). Coplanar electrodes for IL and contact electrodes for MZO films were prepared by depositing Ti (5 nm)/Au (50 nm) using electron-beam-evaporation. Prior to the gating experiment, IL was baked at 80ºC in vacuum to get rid of water contamination: it is known that absorbed water in IL not only affects the performance of EDL layer, but may also modify the surface of gated materials [23, 24]. To avoid the water contamination, the devices were immediately cool down to 230 K in helium or vacuum environment before applying any V_g.

Magnetoresistance and resistance-switching behavior of the devices were measured in a physical property measurement system (PPMS) with a constant current of 1 μA using the four-point-probe geometry. V_g on IL was applied using a Keithley 2400 sourcemeter. Transport measurements in the temperature range of 10 K to 180 K were performed after maintaining V_g for 60 mins at 230 K and removing the V_g at 180 K; since the ionic mobility of IL at 230 K is low, a prolonged duration is required to stabilize the EDL layer. The freezing point of IL used in this work is 210 K, below which the electric field induced in the EDL cannot be dynamically changed. Reheating devices above the freezing point (230 K) is essential to alter the carrier concentration of the MZO surface via the application of V_g.

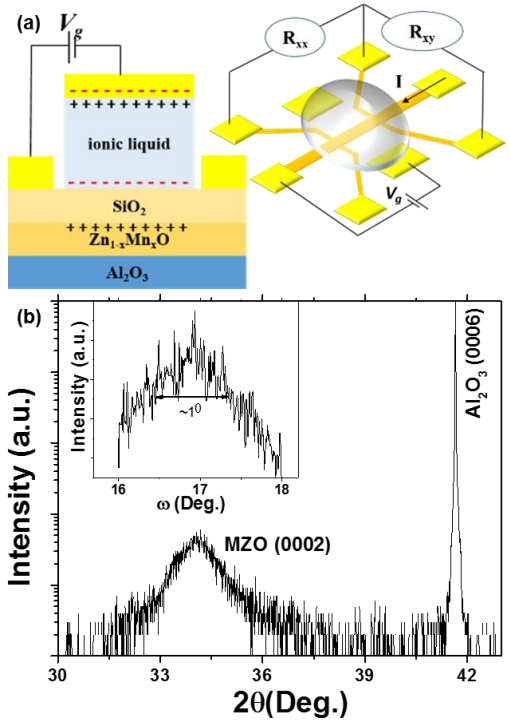

Fig. 1. (a) Schematic diagram of MZO EDLT device (left), and the Hall-bar device configuration with ionic liquid electrolyte as top electrode (right). (b) XRD 2θ scan of 10 nm-thick MZO thin film. Inset: ω-scan of (0002) MZO peak.

III. Results and Discussions

Fig. 1(b) presents the XRD scan of MZO (10 nm) grown on Al_2O_3 (0001) substrate. Only the (0002) diffraction peak of MZO was observed, indicating that highly *c*-axis-oriented MZO films were grown. No impurity phase such as Mn_2O_3, MnO_2 and Mn_3O_4 was observed. The *c*-axis lattice constant (5.26 Å) of the MZO film matches well with the corresponding lattice constant of reported PLD-grown Mn-substituted ZnO films [25, 26]. Fig. 1 (c) shows the XRD ω-scan of (0002) MZO diffraction peak, with a full-width at half-maximum (FWHM) of 1°.

Fig. 2(a) illustrates the V_g-dependent longitudinal resistance (R_{xx}) of MZO EDLT, showing the reversible switching between two distinct resistance levels. The results were collected at 230 K, at which the electrochemical reaction between IL and MZO can be suppressed while the ionic mobility of IL at 230 K is enough to induce accumulation or depletion of electron charge densities at MZO surfaces [27]. ΔR_{xx} increases 33% upon switching V_g from 2 V to -2 V, which is consistent with the scenario of accumulated (depleted) negative charge carriers at the interfaces between IL and MZO [28]. Moreover, the resistance switching behavior in MZO EDLTs exhibits good dynamic response and reversible manipulation via the V_g reversal. Such modulations of R_{xx} are due to electron charge movement in MZO rather than the contribution of gate current: the drain-source current is higher than the gate-source current by at least two orders of magnitude, which is shown in Fig. 2(b).

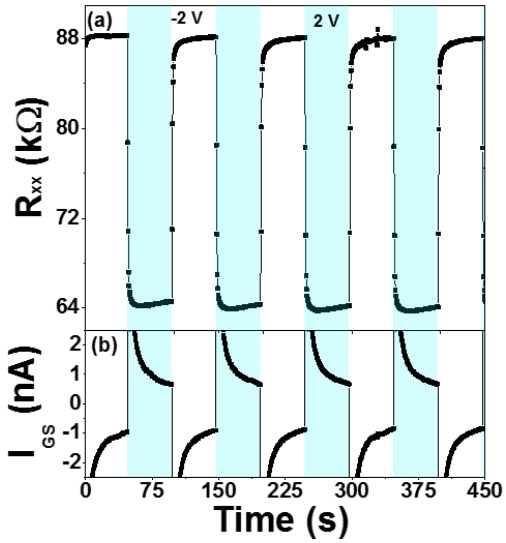

Fig. 2. Time profile of (a) longitudinal resistance (R_{xx}) and (b) gate-source current (I_{GS}) of MZO EDLT with V_g = 2 V (highlighted region) and 2 V.

High- to low-resistance states of MZO EDLT are accompanied by switching V_g from -2 V to 2 V, resulting in the modulation of transport behavior in MZO. To identify that, we carried out measurements of temperature dependent resistivity (ρ) and carrier concentration (η) of MZO EDLTs using the Hall bar configuration. Although a 2-nm SiO_2 protective layer is present in between IL and MZO, the changes in carrier concentration so induced is still much larger

than simply using thick dielectric layers [19, 29]. Fig. 3(a) and (b) show clear correlations of ρ and η of MZO with different polarities of V_g. As the temperature decreases from 180 K to 20 K, the resistivity for +2 V-poled device (ρ(2V)) is smaller than that poled by Vg = -2 V (ρ(-2V)). Regarding the polarity direction of IL switching from +2 V and -2 V, the change in resistivity (Δρ, defines by (Δρ)/ρ=(ρ(2V)-ρ(-2V))/(ρ(-2V)) reaches 3.7 % at 180 K and deceases to 3% at 20 K. Moreover, the Hall coefficient of MZO is negative for all temperatures, implying an electron-doping characteristic of the MZO films. The depletion or accumulation of electron carriers in MZO EDLTs by electric-field effect can be reflected from the change in carrier concentration with different gating voltages.

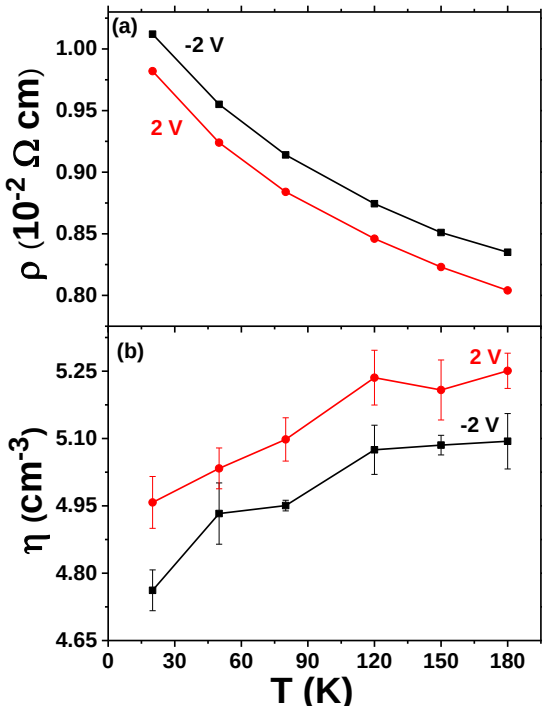

Fig. 3. Temperature dependence of resistivity (a) and carrier concentration (b) with V_g = -2 V (black squares) and 2V (red dots).

To understand the nature of electric-field-induced magnetotranspsort behavior, we focus on the application of V_g in the cooling process. Fig. 4 displays the magnetoresistance (MR) curves with out-of-plane applied field for MZO EDLTs when V_g are set at -2, 0 and 2 V in the cooling process. Here MR is defined as MR=($R_{xx}(H)$-$R_{xx}(0)$)/$R_{xx}(0)$, where $R_{xx}(H)$ and $R_{xx}(0)$ are the R_{xx} values with external magnetic fields of H and zero, respectively. From the comparison in Fig. 4(a), we note that the application of V_g in the cooling process triggers the manipulation of magnetotranspsort at 10 K. When the V_g set to 0 V, the MR exhibits an increasing trend from 0 to 2.8 T, and reaches 0.4% at 2.8 T. The trend of MR becomes a decrease trend from 2.8 to 9 T, and reaches -3% at 9 T. As the negative polarity of V_g is applied, the MR almost traces similar behavior as compared with MR with 0V while the positive MR disappears. After the V_g set 2 V, the change in the peak value of positive and negative MR is observed. The peak positive MR increases from 0 to 1.8% and the negative-MR (measured at 9 T) decreases from –4.5% to -0.6% when V_g increases from -2 to 2 V. As shown in Fig. 4b, negative MR greatly decreases with increasing temperature and become insensitive towards V_g modulations.

The positive MR behaviors at low temperature has been attributed to the spin splitting of *s-d* exchange coupling between carrier and localized electrons conduction band in the DMS, leading to the increase in MR at the low-field regime[30, 31]. On the other hand, the negative MR originates from the interaction between localized electrons and the orbitals of *3d* transition metal ions (Mn^{2+}), which forms the bound magnetic polarons[32]. As the temperature decreases, the localized electron contributing from V_o tends to freeze out, and a hopping channel is established. With certain magnetic field, the random orientation of magnetic polarons tends to align and results in a decrease in resistance of MR measurement. Moreover, negative MR at high-field regime is due to magnetic scattering in 3*d* transition ions, which contributes to the paramagnetic or antiferromagnetic signals. It is well known that not all magnetic ions form magnetic polarons, while some of magnetic ions possess in paramagnetic and antiferromagnetic signal through the mediation of V_o[32].

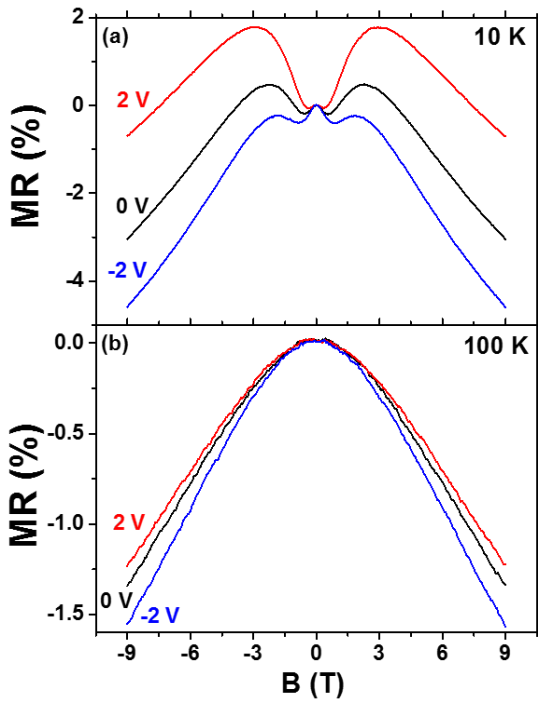

Fig. 4. Magnetoresistance of MZO EDLTs for V_g = -2, 0 and 2 V measured at (a)10 K and (b) 100 K.

Comparing the MR values and change in carrier concentration for different polarity of V_g, an apparent increase in negative MR was observed as the V_g switched from -2 to 2 V. At 10 K, increase in carrier concentration of MZO EDLTs lead to increase the positive MR at low-field regime and decreases the negative MR. The negative MR at T = 100 K, however, only slightly changes upon the V_g reversal from -2 to 2 V. These strong dependences between carrier concentration

and magnetotranspsort is consistent with the previous report in Mn:ZnO film grown on $Pb(Mg_{1/3}Nb_{2/3})O_3$ -$PbTiO_3$ [11]. The impurity band model in DMS proposed by Coey *et al*. that an increase in electron concentration lead to increase the interaction between each polaron, and finally enhance the ferromagnetism in the MZO EDLTs [33]. This increase in ferromagnetism is evidenced by electric-field manipulation in magnetoresistance (T < 100 K). Moreover, the required voltage for manipulating the magnetism in MZO is much less than the previous reports [11, 30, 34]. The present results therefore demonstrate electric-field controllable accumulation/depletion of electron charge carrier in MZO EDLTs through low-voltage gating process, which plays an important role in the manipulation of magnetism in the MZO.

IV. Conclusion

In summary, we fabricated and studied electric-field manipulation of magnetotranspsort properties of MZNO EDLTs via IL gating. Resistance-switching behavior was observed upon the application of different gate voltages, which lead to a reversible control in the transport phenomena at the interface. The MZO EDLTs showed strong dependence between magnetoresistance and V_g. This result also indicated that the ferromagnetism of MZO can be affected by the application of external electric field. Our results suggest that electric-field manipulation through IL gating is a promising method to reversibly control the electrical and magnetic properties of oxide-based materials.

Acknowledgment

This work was supported by HKSAR (PolyU 153015/14P), PolyU (1-ZE25, 1-ZVGH, G-YBPU), and the National Natural Science Foundation of China (Grant No. 51502129).

References

[1] F. Matsukura, Y. Tokura, and H. Ohno, "Control of magnetism by electric fields," *Nat. Nanotech.*, vol. 10, no. 3, pp. 209-220, 2015.

[2] D. Chiba, "Electric field effect on magnetism in metallic ultra-thin films," *Front. Phys.*, vol. 3, no. 83, 2015.

[3] C. Song, B. Cui, F. Li, X. Zhou, and F. Pan, "Recent progress in voltage control of magnetism: Materials, mechanisms, and performance," *Prog. Mater. Sci.*, vol. 87, pp. 33-82, 2017.

[4] M. Liu and N. X. Sun, "Voltage control of magnetism in multiferroic heterostructures," *Philos. Trans. Royal Soc. A.*, vol. 372, no. 2009, 2014.

[5] S. M. Wu et al., "Reversible electric control of exchange bias in a multiferroic field-effect device," *Nat. Mater.*, vol. 9, pp. 756-761, 2010.

[6] H. F. Wong et al., "Enhanced tunability of electrical and magnetic properties in (La,Sr)MnO3 thin films via field-assisted oxygen vacancy modulation," *Solid-State Electron.*, vol. 138, pp. 56-61, 2017.

[7] H. Lu et al., "Electric modulation of magnetization at the $BaTiO_3/La_{0.67}Sr_{0.33}MnO_3$ interfaces," *Appl. Phys. Lett.*, vol. 100, p. 232904, 2012.

[8] T. Kanki, Y.-G. Park, H. Tanaka, and T. Kawai, "Electrical-field control of metal–insulator transition at room temperature in $Pb(Zr_{0.2}Ti_{0.8})O_3/La_{1-x}Ba_xMnO_3$ field-effect transistor," *Appl. Phys. Lett.*, vol. 83, pp. 4860-4862, 2003.

[9] S. Sahoo, S. Polisetty, C.-G. Duan, S. S. Jaswal, E. Y. Tsymbal, and C. Binek, "Ferroelectric control of magnetism in $BaTiO_3$/Fe heterostructures via interface strain coupling," *Phys. Rev. B.*, vol. 76, p. 092108, 2007.

[10] X. Hong, A. Posadas, A. Lin, and C. H. Ahn, "Ferroelectric-field-induced tuning of magnetism in the colossal magnetoresistive oxide La1-xSrxMnO3," *Phys. Rev. B.*, vol. 68, p. 134415, 2003.

[11] Q.-X. Zhu et al., "Ultrahigh Tunability of Room Temperature Electronic Transport and Ferromagnetism in Dilute Magnetic Semiconductor and PMN-PT Single-Crystal-Based Field Effect Transistors via Electric Charge Mediation," *Adv. Funct. Mater.*, vol. 25, pp. 1111-1119, 2015.

[12] W. P. Zhou et al., "Electric field manipulation of magnetic and transport properties in $SrRuO_3/Pb(Mg_{1/3}Nb_{2/3})O_3$-$PbTiO_3$ heterostructure," *Sci. Rep.*, vol. 4, p. 6991, 2014.

[13] B. Cui et al., "Reversible Ferromagnetic Phase Transition in Electrode-Gated Manganites," *Adv. Funct. Mater.*, vol. 24, pp. 7233-7240, 2014.

[14] C. Ge et al., "Metal–Insulator Transition Induced by Oxygen Vacancies from Electrochemical Reaction in Ionic Liquid-Gated Manganite Films," *Adv. Mater. Interfaces.*, vol. 2, p. 1500407, 2015.

[15] D. Passarello, S. G. Altendorf, J. Jeong, M. G. Samant, and S. S. P. Parkin, "Metallization of Epitaxial VO_2 Films by Ionic Liquid Gating through Initially Insulating TiO_2 Layers," *Nano Lett.*, vol. 16, pp. 5475-5481, 2016.

[16] H. Ji, J. Wei, and D. Natelson, "Modulation of the Electrical Properties of VO2 Nanobeams Using an Ionic Liquid as a Gating Medium," *Nano Lett.*, vol. 12, pp. 2988-2992, 2012.

[17] H. T. Yi, B. Gao, W. Xie, S.-W. Cheong, and V. Podzorov, "Tuning the metal-insulator crossover and magnetism in $SrRuO_3$ by ionic gating," *Sci. Rep.*, vol. 4, p. 6604, 2014.

[18] J. Shiogai, Y. Ito, T. Mitsuhashi, T. Nojima, and A. Tsukazaki, "Electric-field-induced superconductivity in electrochemically etched ultrathin FeSe films on $SrTiO_3$ and MgO," *Nat. Phys.*, vol. 12, pp. 42-46, 2016.

[19] Y. Wang et al., "Electrical Control of the Exchange Spring in Antiferromagnetic Metals," *Adv. Mater.*, vol. 27, pp. 3196-3201, 2015.

[20] X. L. Wang, K. H. Lai, and A. Ruotolo, "A comparative study on the ferromagnetic properties of undoped and Mn-doped ZnO," *J. Alloys Compd.*, vol. 542, pp. 147-150, 2012.

[21] X. L. Wang et al., "Effect of the magnetic order on the room-temperature band-gap of Mn-doped ZnO thin films," *Appl. Phys. Lett.*, vol. 102, p. 102112, 2013.

[22] J. Hüpkes, J. I. Owen, S. E. Pust, and E. Bunte "Chemical Etching of Zinc Oxide for Thin-Film Silicon Solar Cells," *ChemPhysChem*, vol. 13, pp. 66-73, 2012.

[23] H. Yuan, H. Shimotani, A. Tsukazaki, A. Ohtomo, M. Kawasaki, and Y. Iwasa, "Hydrogenation-Induced Surface Polarity Recognition and Proton Memory Behavior at Protic-Ionic-Liquid/Oxide Electric-Double-Layer Interfaces," *J. Am. Chem. Soc.*, vol. 132, pp. 6672-6678, 2010.

[24] T. D. Schladt et al., "Crystal-Facet-Dependent Metallization in Electrolyte-Gated Rutile TiO2 Single Crystals," *ACS Nano*, vol. 7, pp. 8074-8081, 2013.

[25] Q. Shao et al., "Chemical states and ferromagnetism in heavily Mn-substituted zinc oxide thin films," *J. Appl. Phys.*, vol. 115, no. 15, p. 153902, 2014.

[26] T. Fukumura, Z. Jin, A. Ohtomo, H. Koinuma, and M. Kawasaki, "An oxide-diluted magnetic semiconductor: Mn-doped ZnO," *Appl. Phys. Lett.*, vol. 75, pp. 3366-3368, 1999.

[27] J. Walter, H. Wang, B. Luo, C. D. Frisbie, and C. Leighton, "Electrostatic versus Electrochemical Doping and Control of Ferromagnetism in Ion-Gel-Gated Ultrathin $La_{0.5}Sr_{0.5}CoO_{3-\delta}$," *ACS Nano*, vol. 10, pp. 7799-7810, 2016.

[28] H. Yuan, H. Shimotani, A. Tsukazaki, A. Ohtomo, M. Kawasaki, and Y. Iwasa, "High-Density Carrier Accumulation in ZnO Field-Effect Transistors Gated by Electric Double Layers of Ionic Liquids," *Adv. Funct. Mater.*, vol. 19, pp. 1046-1053, 2009.

[29] D. Chiba and T. Ono, "Control of magnetism in Co by an electric field," *J. Phys. D*, vol. 46, p. 213001, 2013.

[30] L.-T. Chang et al., "Electric-Field Control of Ferromagnetism in Mn-Doped ZnO Nanowires," *Nano Lett.*, vol. 14, pp. 1823-1829, 2014.

[31] K. R. Sapkota, W. Chen, F. S. Maloney, U. Poudyal, and W. Wang, "Magnetoresistance manipulation and sign reversal in Mn-doped ZnO nanowires," *Sci. Rep.*, vol. 6, p. 35036, 2016.

[32] X. L. Wang et al., "Giant negative magnetoresistance in Manganese-substituted Zinc Oxide," *Sci. Rep.*, vol. 5, p. 9221, 2015.

[33] J. M. D. Coey, M. Venkatesan, and C. B. Fitzgerald, "Donor impurity band exchange in dilute ferromagnetic oxides," *Nat. Mater.*, vol. 4, pp. 173-179, 2005.

[34] V. Modepalli et al., "Gate-Tunable Spin Exchange Interactions and Inversion of Magnetoresistance in Single Ferromagnetic ZnO Nanowires," *ACS Nano*, vol. 10, pp. 4618-4626, 2016.